

De-IReps: Searching for improved Re-parameterizing Architecture based on Differentiable Evolution Strategy

Xinyi Yu, Xiaowei Wang, Mingyang Zhang, Jintao Rong, Linlin Ou

Abstract

In recent years, neural architecture search (NAS) has shown great competitiveness in many fields and re-parameterization techniques have started to appear in the field of architectural search. However, most edge devices do not adapt well to networks, especially the multi-branch structure, which is searched by NAS. Therefore, in this work we design a search space that covers almost all re-parameterization operations. In this search space, multiple-path networks can be unconditionally re-parameterized into single-path networks. Thus, enhancing the usefulness of traditional nas. Meanwhile we summarize the characteristics of the re-parameterization search space and propose a differentiable evolutionary strategy (DES) to explore the re-parameterization search space. We visualize the features of the searched architecture and give our explanation for the appearance of this architecture. In this work, we can achieve efficient search and find better network structures. Respectively, we completed the architecture search on CIFAR-10 with the test accuracy of 96.64% (IrepResNet-18) and 95.65% (IrepVGG-16) and on ImageNet with the test accuracy of 77.92% (IrepResNet-50).

1. Introduction

In recent years, convolutional neural networks (CNNs) have shown their powerful feature representation capabilities in computer vision problems, such as target detection [1, 2], semantic segmentation [3, 4], image recognition [5], image generation [6], and target re-recognition [7,8]. Early convolutional neural networks, such as VGG [9], ResNet [10], MobileNet [11-13], DenseNet [14], etc., were designed based on a priori knowledge. Neural architecture search [15-22], inspired by the early networks, attempts to reduce the

reliance on prior knowledge and automatically search for the optimal network to achieve the best feature extraction capability. However, most of the current architectures searched by nas are multi-branch architectures and cannot be well adapted to edge devices when landing. As a result, it is difficult to implement traditional nas for end-to-end applications. Based on the issues, we have reconsidered the problem of neural network architecture search. Since the edge devices are well adapted to ResNet, VGG etc., we use the traditional ResNet as our search framework, in which all the 3×3 operations are replaced with our re-parameterized search space. Then re-parameterizing the searched multi-branch ResNet into the original structure to ensure the practicality of the network on the edge devices while further improving the performance of the ResNet network.

Neural structure search mainly consists of three parts: search strategy, search space and evaluation strategy. In general, in terms of the hierarchy of search strategies, we can classify them into reinforcement learning (RL) based, evolutionary algorithms (EA) based, and gradient-based. Reinforcement learning-based architectures search [23-25] uses reinforcement learning algorithms to generate better networks by optimizing controllers. Evolutionary algorithm-based architecture search [19, 21, 26, 27] samples and evaluates the performance of subnets from a supernet, relying on genetics, variation, and crossover to drive the algorithm to convergence. DARTS [15] uses a differentiable method to train the Supernet and retain some operations with higher weight of the network to constitute the best architecture. This approach allows the network to converge much faster, significantly reducing search time and computational resources. A very competitive network can be found in 4 GPU days compared to hundreds of GPU days.

The structural re-parameterization technique [28-30] has been used to improve the performance of network models. It combines several different operations into one operation. RepNAS [31] proposed a re-parameterized search space in which all multi-branch structures can be re-parameterized into single-branch structures. The re-parameterized structural improves the forward inference speed of the network while keeping the performance of the network unchanged, which is very competitive when deployed on edge devices.

In this paper, we efficiently search the structural re-parameterization search space by the "Differential Evolutionary Strategy" (DES) approach. During deployment, the searched network structures can be reparameterized into individual branch architectures. Specifically, the strategy efficiently searches for architectures in a re-parameterized search space during the search process and directly ignores bad architectures. In addition, we use the parameter batch adaptive update method to optimize the SuperNet to further accelerate the convergence of the network and reduce the gap between networks. Our contributions can be summarized as follows:

- We propose a differentiable evolutionary algorithm that improves the problem of slow convergence in the genetic variation phase due to the non-directed nature of the evolutionary strategy. Meanwhile, our search method can effectively explore more architectures in the search space of structural re-parameterization.
- We designed an "age" function that better balances the training imbalance between the old and new architectures in the population. It also avoids the problem of retaining some architectures in the population for too long.
- We extend the re-parameterized search space to include all operations that can be re-parameterized. In the evaluation phase, we re-parameterized the multi-branch architecture into a single-branch architecture, which saving significant time in verifying the performance of the networks.

2 Related Work

2.1 Network Architecture Search

Neural architecture search (NAS) is a technique that is widely used in many fields to match the appropriate task to the best network structure. Early NAS were accomplished through reinforcement learning. It took hundreds of GPU days to train an agent that could generate superior architecture. To speed up the search, ENAS [25] introduced a weight-sharing method that improved the search speed by thousands of times. In addition, Bayesian algorithms [32, 33] achieve accelerated architecture search by varying hyperparameters, such as the number of cells and reserved candidate operations, the size of the convolution kernel, the parameter learning rate etc. EA-based approaches [19, 21, 22, 34] search for architectures with the help of evolutionary algorithms, which rely on fitness selection mechanisms, variation, and genetic methods to search for globally optimal architectures in convex spaces.

Gradient-based neural architecture search benefits from the introduction of differentiable functions, which transform the discrete search space into continuous so that it can be optimized by means of gradients [15, 16, 18, 20, 36]. It achieves the search for the optimal structure by balancing the weight parameters of the network and the architecture parameters. From the perspective of parameter optimization, it can be divided into two categories. One is bilevel optimization [15, 20, 36], which optimizes the architecture with the weight parameters of the network are optimal. The other is one-level optimization [16, 37], which regards the weight of network and architecture optimization as independent processes. The gradient-based method improves the search speed and a competitive architecture can be searched with only a few GPU days.

However, gradient-based methods can easily lead to poor correlation between the search phrase and the evaluation phase. Several works [38, 39] have also demonstrated this problem experimentally and have adapted the search space as well as the search strategy thus enhancing the relevance of the architectures. Gradient-based architecture search also introduces selection preferences, which leads to a limited exploration of the diversity of network structures during the search. For these problems, it's necessary to address them from a novel perspective.

2.2 Structural Re-parameterization

The structural reparameterization technique is an equivalent structural transformation that can equivalently convert a multi-branch architecture into a single-branch architecture to obtain faster reasoning. ACNet [28] proposes to fuse 1D asymmetric convolution into square convolution to enhance the feature representation capability of square convolution. DDB [29] aims to enhance the representation of a single convolution by combining diverse branches, and give methods for fusing multiple convolution operations in various combinatorial forms. RepVGG [30] constructs a residual structure-like branch base on the VGG network and fuses the trained residual-like structure into a 3×3 convolution by structural reparameterization technique. The structural re-parameterization technique not only gives the network a faster inference speed, but also maintains the same performance as a multi-branch network. Structural reparameterization techniques can fuse parallel structures with each other, in addition to combined operations for other cases, such as Conv-BN to Conv, Sequence Conv structure to Conv, a Conv for depth concatenation to a Conv, $K \times K$ average pooling to $K \times K$ Conv. In this work, we use the above-mentioned re-parameterization technique to implement the structural reparameterization.

3. PROPOSED APPROACH

3.1 SuperNet of dereps

Any sub-architecture in the re-parameterized search space can be converted from multi-branch architectures to single branch architectures by re-parameterization technology. The search space of RepNAS [31] is built based on VGG network, which is composed by blocks. Each block is composed of multiple independent operations O_k . Therefore, the output characteristics of each block can be described as $x_i = \sum_{k=0}^n o_k \cdot (x_j)$.

By studying the re-parameterized search space, we summarize two characteristics of the search space, which can be described as follows:

- a) The number of parameters of the network in the structural reparameterization search space is only

related to the number of channels. Therefore, changing the number of branches in the cell and the number of operation stacks only affect the resource consumption of training, not the size of the re-parameterized network and the speed of inference.

- b) In the reparameterized search space, for convolutions with the same group but different kernel sizes, the weight parameters of convolutions can be fused into the other convolutions if the centers of the convolution kernels can be exactly overlapped.

In this work, in addition to the 3×3 , 1×3 , 3×1 , 1×1 , 1×1 , 3×3 convolution operations, average pooling operation and skip connect operation, we also add 1×2 , 2×1 and 2×2 dilation convolution to the search space of RepNAS. Dilation convolution can be perfectly transformed into 3×3 convolution. Specifically, it can be expressed by following equation:

$$F_{::,1:2,::2}^{3 \times 3} = F_{::,::}^{1 \times 2} \quad (1)$$

$$F_{::,::2,1:2}^{3 \times 3} = F_{::,::}^{2 \times 1} \quad (2)$$

$$F_{::,::2,::2}^{3 \times 3} = F_{::,::}^{2 \times 2} \quad (3)$$

Where $F^{3 \times 3}$ represents 3×3 convolution with weights of zero, $F^{1 \times 2}$, $F^{2 \times 1}$ and $F^{2 \times 2}$ represent 1×2 , 2×1 and 2×1 dilation convolution. According to our motivation, we replace the 3×3 convolution in ResNet with the re-parameterized search space that we designed.

3.2 Adaptive batch optimization of parameters

Since we use evolutionary algorithms to search for architectures, we use binary encoding (0 & 1) to cover the supernet to obtain different subnet. The element 1 indicates participation in forward propagation and 0 indicates non-participation. To avoid unbalanced training of architecture parameters and weight parameters due to sampling in the search process. We introduce the method of batch optimization of parameters. It can be expressed as:

$$d\omega = \frac{1}{P} \sum_{i=1}^P d\omega_i = \frac{1}{P} \sum_{i=1}^P \frac{\partial L_i}{\partial \omega} \odot \mathcal{M}_i \approx \frac{1}{B} \sum_{j=0}^B \frac{\partial L_{\mathcal{M}_j}}{\partial \omega_{\mathcal{M}_j}} \quad (4)$$

Where P represents the number of populations. B is the number of subnet, which is randomly sampled from the population. Eq. (4) shows that the weight parameters of supernet can be optimized by updating the gradients of all subnet in the population in batch. Further it can be approximated as the average gradients of a part of the individuals in the population. However, it is unbalance that each individual updating $1/B$ of the original gradient value.

We believe that the difference of network performance should be dominated by the difference of architecture, not caused by the difference of the parameters. Therefore, to reduce the unfairness, we optimize the parameters according to the loss value of the architecture output and quantified it by the Softmax function. So, it can be written:

$$p_{S_j} = \frac{L_{S_j}}{\sum_{S \in S} \exp(L_S)} \quad (5)$$

Where S represents the architecture sampled from the population and L_S means the loss value of architecture s . Taking Eq. (5) into Eq. (4), we can get the following equation:

$$d\omega = \sum_{j \in S} \frac{L_{S_j}}{\sum_{S \in S} \exp(L_S)} \cdot \frac{\partial L_{\mathcal{M}_j}}{\partial \omega_{\mathcal{M}_j}} \quad (6)$$

Through the equation, we make the impact of architecture on performance dominant in the search process.

We use one-level method to optimize parameters on the training dataset \mathcal{D}_{train} . In the process of architecture search, we limit the number of branches of the generated sub-architecture to less than C and make all sub-architectures share the weight parameters of supernet to accelerate the convergence speed of supernet. Therefore, the search process can be given as:

$$\omega_{t+1} = \omega_t - \xi_\omega \cdot \sum_{j \in S} \frac{L_{S_j}}{\sum_{S \in S} \exp(L_S)} \cdot \frac{\partial L_{train\mathcal{M}_j}}{\partial \omega_{\mathcal{M}_j}} \quad (7)$$

$$s.t. \begin{cases} \theta_{t+1} = \theta_t - \xi_\theta \cdot \nabla_\theta \mathcal{L}(\omega_t, \theta_t; \mathcal{D}_{train}) \\ \mathcal{M} = S_{\{\mathcal{M}_1, \mathcal{M}_2, \dots, \mathcal{M}_P\}} \\ |\mathcal{M}_j| \leq C \end{cases} \quad (8)$$

Where θ and ω is the architecture parameter and the weight parameter of the network.

3.3 Selection method of Architecture

Many previous neural architecture search methods based on evolutionary algorithms using naive mutation, crossover and genetic operations to explore architectures. Meanwhile, the network with the best performance in the population will be retained and used as the parent network for subsequent operation. In this way, the algorithm tends to converge gradually as a whole. However, using naive evolutionary operation will slow down the convergence process of the algorithm to a great extent. Therefore, we introduce differentiable methods to learn the importance of blocks and operations, as shown in Figure 1. The dotted line indicates not participating in the forward propagation process and the solid line indicates participating in the forward propagation process. A block consists of multiple candidate operations $O_p(\cdot)$.

We use Sigmoid function to quantify the block parameters β and operation parameters α . Therefore, the output characteristics of the block can $\bar{B}^i(x)$ be expressed as:

$$\bar{B}^i(x) = \beta'_i \sum_{o \in O} \frac{1}{1 + e^{-\alpha'_o}} B(x) + F(x) \quad (9)$$

$$\beta'_i = \frac{1}{1 + e^{-\beta_i}} \quad (10)$$

Where B is the number of blocks in search space. $F(x)$ is the feature map of the fixed operation.

Based on the above, we add random disturbances to the architecture parameters α and β to ensure the diversity of the architecture when generating the sub-generation architectures. We define the disturbance range as:

$$\sigma_\alpha \in \left(\frac{1}{1 + e^{-\alpha_0}} - \max\left(\frac{1}{1 + e^{-\alpha}}\right), \frac{1}{1 + e^{-\alpha_0}} - \min\left(\frac{1}{1 + e^{-\alpha}}\right) \right) \quad (11)$$

$$\sigma_\beta \in \left(\frac{1}{1 + e^{-\beta_0}} - \max\left(\frac{1}{1 + e^{-\beta}}\right), \frac{1}{1 + e^{-\beta_0}} - \min\left(\frac{1}{1 + e^{-\beta}}\right) \right) \quad (12)$$

Respectively, σ_α and σ_β is random disturbance. α_0 and β_0 are the initialization weights of α and β , respectively, which we consider as baselines for the importance of operations and blocks. We take the deviation of the maximum and minimum weight values from the baseline as the range of perturbation.

In the generation phase of the sub-architecture, we complete it in two steps. Firstly, select the block

according to the value of $\beta'_i + \sigma_\beta$. Secondly, the value of $\alpha'_i + \sigma_\alpha$ determines whether the operation needs to be retained. This process can be simply described as:

$$\begin{cases} 1, & \text{if } \text{rank}[(\beta'_i + \sigma_\beta) \cdot (\alpha'_i + \sigma_\alpha)] \leq C \\ 0, & \text{else} \end{cases} \quad (13)$$

Where 1 means reserved and 0 is not reserved. C represents the number of the operations, which is reserved. $\text{rank}(\cdot)$ denotes the global ranking. We rank $(\beta'_i + \sigma_\beta) \cdot (\alpha'_i + \sigma_\alpha)$ globally and retain the top C operations.

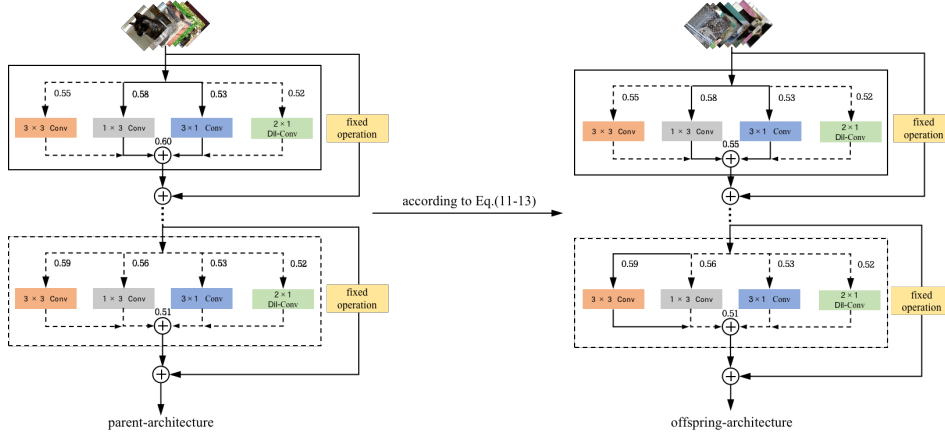


Fig 1. **Left:** Sampling from Supernet to obtain the parent architecture and training it. The output features of each operations need to be multiplied by the weight of the block. We keep the option that maximizes the expression of fixed operational features. **Right:** The trained parent architecture generates the offspring architecture according to Eq. (11-13)

architecture to balance the training imbalance between the offspring architecture and the parent architecture, such as CARS [21] and AmoebaNet [40]

For the issues mentioned above, we design a function, which has the following characteristics. a) It can give appropriate penalties to the architecture with more training times. b) Assuming that the feature of the architecture in the population is completely inherited by offspring generations after a epochs, this function can weed out the architecture from the population. According to the requirements, we come up with a loss function, formally as:

$$\varphi(\mathcal{E}) = \eta \left(\frac{1}{\mathcal{E} - a - \mu} - \log_a(\mathcal{E}) \right) \quad (14)$$

Where η is the scale factor. The parameter a determines the turning point of the function, as shown in figure 2. \mathcal{E} represents the number of epochs that the

3.4 Performance Estimation of Architecture

3.4.1 Solve the diversity Architecture

The networks with great performance can generate offspring architectures and participate in the training of next epochs when using evolutionary strategy to search sub-networks. However, the excellent architectures are retained in the population for a long time will make the lack of diversity of group architectures. Therefore, many works not only evaluate the accuracy of the architecture, but also consider the age attribute of the

architecture has survived and μ can appropriately adjust the decline rate of the curve. So, the value range of μ is $(0, \eta/(1 - \eta))$. We regularize the accuracy of the architecture, which can be expressed as:

$$\mathcal{S}_i = \mathcal{A}_{i \in P} + \varphi_{i \in P}(\mathcal{E}) \quad (15)$$

Where \mathcal{A}_i is the performance of the network on the verification dataset, $0 \leq \mathcal{A}_i \leq 1$. Through the regularization of \mathcal{A}_i , we obtain the comprehensive performance of each architecture.

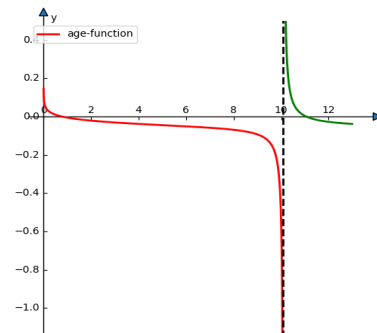


Fig 2. The figure shows the function image when $\alpha = 10$, $\mu = 0.1$ and $\eta = 0.05$. We intercept the function curve in the red part as the regularization function.

3.4.2 Fast acquisition of Architecture Performance

Based on the idea of re-parameterized architecture, we re-parameterize the architecture of multi-branch into the architecture of single branch. After re-parameterized, the network has only 3×3 operation and nonlinear operation, so it greatly speeds up the performance evaluation process of the network and reduces the consumption of computing resources. In addition, in experiments, we found that although the performance of the reparameterized architecture does not change, there is still a very small accuracy error compared to before the reparameterization. Therefore, this verification method of ours also eliminates this error.

In the search stage, we use α and β to characterize the importance of each blocks and candidate operations. After the architecture is re-parameterized, the weight and bias value of the re-parameterized convolution need to be scaled to $\alpha \cdot \beta$ times to ensure that the performance of the architecture remains unchanged. Table 1 shows the time consumption of the verification process on CIFAR-10. Respectively, we set the number of populations to [64, 128, 256]. Our approach increases the speed of the architecture evaluation by around 60% compared to the original evaluation method. In this experiment, we set the population size to 128, considering factors such as population diversity and search time.

4. Experiments

We expand the re-parameterized search space to achieve better results. In order to verify that the re-parameterized search space is effective for different data sets, we searched the architecture on CIFAR-10 and ImageNet-1K respectively. We fix the 3×3 convolution and search for the other convolution operations during the search. Our experiment is divided into two stages: search stage and retraining stage.

4.1 Searching Architectures on CIFAR-10

We replace the 3×3 convolution in VGG-16 and ResNet18 into our re-parameterization search space respectively. The hyper-parameter of the network is followed with ACNet [28] and Resnet [10]. The population is 128. As shown in Table 1, the re-parameterized architecture can obtain the maximum speed-up rate in the verification stage when the number of populations are 128. We use the SGD optimizer with the learning rate of 0.1 to optimize the parameters of the network. To optimize the architecture parameters α , β , we all use Adam optimizer with learning rate of 0.03 and (0.5, 0.999) betas. Based on the experimental proof of RepNAS, we keep 2/3 of the number of branches in the search space. We train the parameters with 10 epochs. In the training process, we sample 5 sub-architectures to update the parameter of supernet. In the process of evolution, we all mutate and cross the structures of the architecture with a probability of 0.5. For the age function, $\eta = 0.05$, $\alpha = 10$, $\mu = 0.01$.

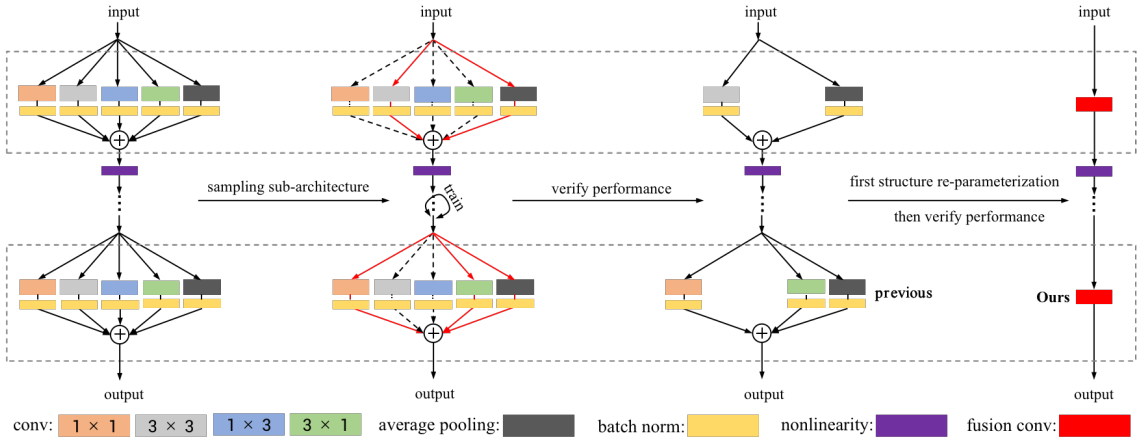


Fig3. Using the re-parameterized structure to obtain the accuracy. Each sub-architecture structure in the population is different from each other, but the re-parameterized structure can become the structure of the rightest architecture.

Model	Population Size/Time		64/S	128/S	256/S
	Multi-Branch	VGG-16	1349.4	2681.1	5336.9
		Resnet-18	649.1	1301.6	2685.7
	Re-Parameterized	VGG-16	499.5	1000.0	1823.9
		Resnet-18	286.3	571.5	1133.9
	Acceleration percentage (%)	VGG-16	63.7	62.7	65.8
		Resnet-18	55.9	56.1	57.8

Table 1. We obtain the performance architectural on Nvidia A100 GPU. In the table, we regard the time spent in transforming the architecture into a single path structure as part of the time spent in the verification stage. The results are average of verifying 10 generations and the batch size is 512, full precision(fp32).

Algorithm 1 Adaptive differentiable evolution strategy for neural architecture search

Input: SuperNet \mathcal{N} , Population $P = \{P_1, \dots, P_k\}$, offspring expand ratio t , evolution number E_{evo} , Warm up number E_{warm} , parameter optimization epochs E_p , arch-parameters β , parameters of the regularization function $\{a, \mu, \eta, \mathcal{E}\}$.

```

1: while  $i < E_{warm}$  do:
3:   Warm up SuperNet  $\mathcal{N}$ 
4: end while
5: while  $j < E_{evo}$  do:
6:   while  $k < E_p$  do:
7:     for Mini-batch data  $X$ , target  $Y$  in Dataset
8:       Random sample  $B$  sub-architectures.
       from Population.
9:       Forward  $B$  sampled sub-networks
10:      Calculate loss and compute the gradients
       according to Eq. (4)-Eq. (6).
11:      Update the network parameters  $W$  and
       architecture parameters  $\alpha, \beta$ .
12:    end for
13:  end while
14:  Re-parameterize architecture and obtain the
    performance of the architecture.
15:  Select the architecture according to Eq. (15)
    and generate other offspring architectures
    according to Eq. (11-13).

```

16: **end while**

Output: Architectures $P = \{P'_1, \dots, P'_k\}$.

We search for 500 epochs and retrain some architectures on Cifar-10. Except for the learning rate and the probability of the droppath, the training process and the other parameter setting are the same as DARTS [15], we set the learning rate and the probability of randomly discarding the path to 0.05 and 0.08 respectively.

Table 2 shows the comparison between our results and related work. We fix the “skip-connect” and 3×3 convolution in the supernet respectively and search other candidate operations. Our Supernet is based on AcNet [28] and ResNet [10]. We achieved 1.02% better accuracy than RepVGG [30] and 0.21% than RepNAS. The architecture we searched has great advantages in the reasoning process, especially in the processing speed of single image.

4.2 Experience on ImageNet

To reveal the generalization ability, we evaluate IRepesNet on the ImageNet-1K, which contains 1.3M images for training and 50K for validation from 1000 classes. To save computational resources and speed up the search, based on the conclusion of ACNet [28], we remove the 2×2 separable convolution from the search space. Meanwhile, we fix the 3×3 convolution operation during the search. We use Nvidia A100 to train the models, $B = 1$, $E_{warm} = 5$ and the batch size is 256. We search the architecture for 100 epoch and then fixed the structure of the supernet to continue training for 120 epochs. We use Adam optimizer with 0.0001 learning rate and (0.5, 0.999) betas to optimize

Model	Top-1 (%)	Params(M)	Inference (ms)	Search Cost (GPU days)	Search Method
VGG	94.12	14.73	2.14	—	—
ResNet-18	96.21	11.69	4.12	—	—
RepVGG	94.62	14.73	1.76	—	—
AcNet	94.47	14.73	1.76	—	—
DARTS (second)	97.24	3.3	31	4	gradient-based
P-DARTS	97.5	3.4	33	0.3	gradient-based
RepNAS (VGG)	95.43	11.69	1.76	0.7	gradient-based
GoldNAS	97.39	3.67	40	1.1	gradient-based
CARS	97.38	3.6	27	0.4	Evolution
AmoebaNet-A	96.60	3.2	38	3150	Evolution
IRep-Resnet18	96.61	11.69	3.93	8.0	Evolution
IRep-Vgg16	95.65	14.73	1.76	16.0	Evolution

Table 2. Comparison with state-of-the-art image classifiers on CIFAR-10 dataset. We calculated the parameters of the model and tested the model of the inference time on Nvidia A100 GPU with a batch of 1, full precision(fp32).

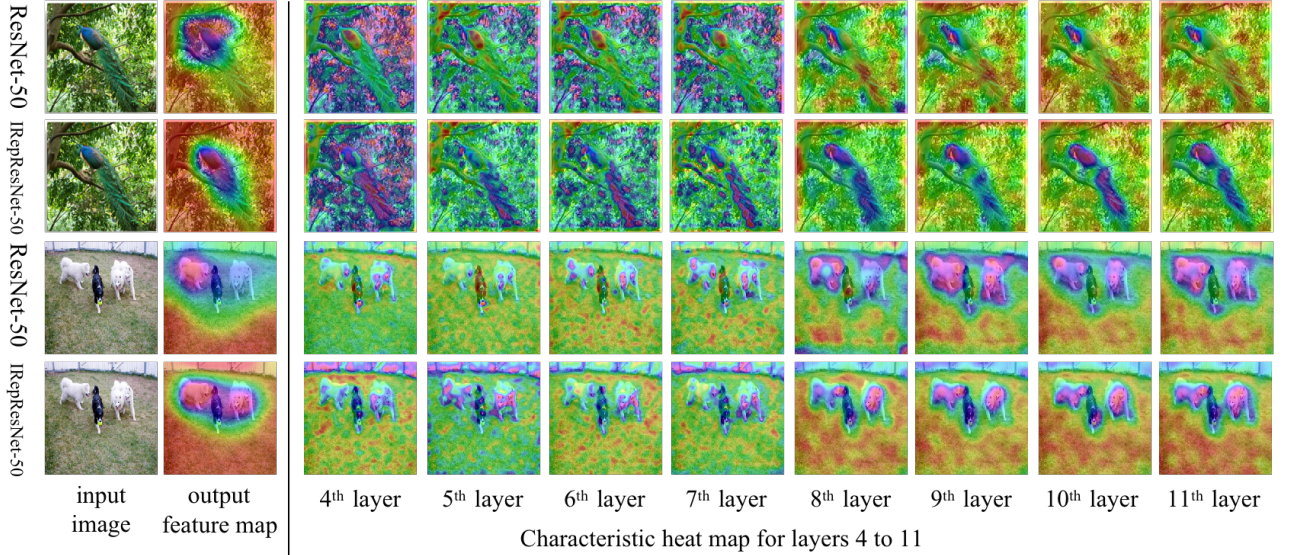


Fig3. We visualized the output feature values of the convolution in the ResNet-50 and IrepResNet-50 network to better interpret the structure of our architecture. We consider the structure of $\text{Conv}1 \times 1 - \text{conv}3 \times 3 - \text{conv}1 \times 1$ as one layer. The first and second columns are the original image and the heat map of the last layer of convolution output features. The other columns are the heat maps of the feature outputs convolved in the fourth layer to the 11th layer. IRepresNet-50 has significantly better feature focus than ResNet-50.

α , β and reserve 1/2 of the number of branches. We set $\eta = 0.05$, $a = 5$, $\mu = 0.01$. The other super parameters are the same as CARS [21].

We compare the searched architectures with state-of-the-arts in Table 3. Compared to others, ours (IrepResNet-50) also shows favorable performance. We achieved a top-1 accuracy of 77.92%, which is 1.82% higher than ResNet-50, 0.84% higher than DyRep [41] and 1.21% higher than DDB. Meanwhile, our architecture has a faster inference speed compared to ResNet-50, DARTS, P-DARTS, GoldNAS, etc.

We plot the Irepresnet-50 architecture in the **appendix**. The Irepresnet-50 architecture appears truncated in the middle, i.e., the first eight layers (one operation is excluded in the eighth layer) retain all enhancement operations, and the last eight layers (one operation is retained in the ninth layer) exclude all enhancement operations. To better explain this phenomenon, we visualized the middle layer feature maps of ResNet-50 and IRepResNet-50, as shown in Figure 4. The above figure visualizes the feature regions that IRepResNet-50 and ResNet50 focus on. It can be concluded from the visualization that IRepResNet50 is more discriminative and precisely focused on the target

compared to ResNet50. We compare the feature visualization of the convolutional layers and find that for the ResNet, the role of its first eight layers of convolution is mainly to achieve the separation of foreground and background in the image. While the second eight layers of convolution are mainly to further distinguish the foreground from the background and focus on the target in the image. This division of tasks is significant for resnet50, where the first eight layers obtain less feature information because of the small number of channels, then the re-parameterization operation is more important to enhance the acquisition of feature information currently, which make the re-parameterization operations have greater weight. The latter eight layers can acquire more feature information due to the large number of channels, allowing them to take on the task of focusing on the target and refining the foreground and background in the picture. Compared with the first eight layers, the re-parameterization operation has an insignificant gain effect on them and has a little weight. Therefore, the search architecture under resource constraints makes the algorithm prefer to retain the re-parameterization operations in the first eight layers.

Model	Top-1(%)	Top-5(%)	Params(M)	Inference (ms)	Search Cost (GPU-days)	Search Method
ResNet-50	76.10	93.29	25.56	38.8	—	—
DyRep	77.08	—	25.56	15.6	—	—
DDB	76.71	—	25.56	15.6	—	—
DARTS (second)	73.30	91.3	4.7	67.4	4	gradient-based
P-DARTS	75.60	92.6	4.9	62.3	0.3	gradient-based
GoldNAS	76.10	92.7	6.4	39.4	1.7	gradient-based
CARS	75.20	92.5	5.1	59.9	0.4	evolution
AmoebaNet-B	74.50	92.0	5.1	218	3150	evolution
Ours (IRep-Resnet50)	77.92	93.88	25.56	15.6	30	evolution

Table 2. De-IREps performance on ImageNet with comparisons to other NAS methods and models. All experiments on the ImageNet were performed based on Nvidia A100 GPU. We calculated the parameters of the model and tested the model of the inference time with a batch of 1, full precision(fp32).

4.3 Ablation Study

I. Remove age function from De-IREps

The introduction of age functions can increase the diversity of architectures in the search process and we have empirically justified the effectiveness of De-IREps. In this partial, we explore it through ablation experiments to explore the extent to which this regular term affects the final searched architecture.

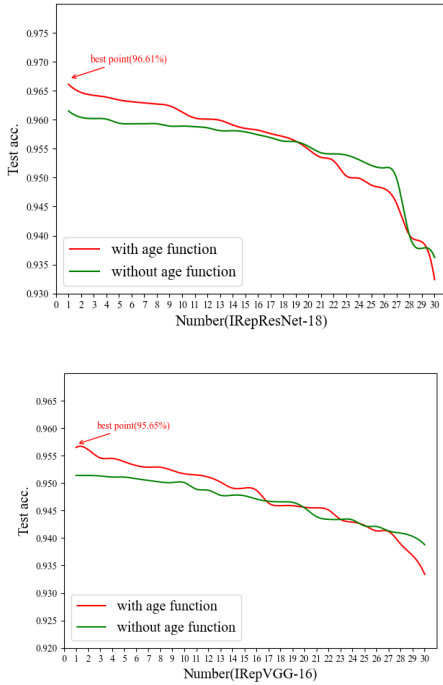


Fig 4. Results of age-functional ablation experiments. We randomly select 30 architectures from the output population and retrain them to obtain the results in Figure 3. In terms of the overall trend, the final population will contain better architectures driven by the age function.

II. Searching under different resource constraints

To explore the impact of the evolved reparameterised search space on the performance of the architecture under different resource constraints, we performed an architectural search on the cifar-10 dataset for VGG-16 and ResNet-18 under different resource constraints. Specifically, we searched for $[1/6, 1/3, 1/2, 2/3, 5/6, 1]$ times the total number of

branches in the search space, respectively, and obtained the results in the table. When the resource constraint reaches $2/3$ times the total number of branches, the searched architecture achieves a better performance. This is extremely similar to the experimental results derived by RepNAS. Our analysis suggests that the main reason for this may be that our addition of the separable convolution operation has a weaker or approximately equal enhancement effect on the 3×3 convolution than the $1 \times 3, 3 \times 1$, etc. convolution [28]. If the same number of branches as in repnas is guaranteed, some of the $1 \times 3, 3 \times 1$, etc. convolutions will be replaced by separable convolutions, which will result in an architecture with performance similar to or even weaker than the RepNAS architectures.

Model	1/6	1/3	1/2	2/3	5/6	1
IRep-VGG16	94.22	94.58	95.40	95.65	95.64	95.64
IRep-ResNet18	96.28	96.47	96.47	96.61	95.50	96.52

Table 4. Performance of the architecture on the CIFAR-10 dataset under different resource constraints.

5. Conclusion

In this paper, we propose a differentiable evolutionary algorithm, which is used to search the improving re-parameterized search space. Compared with other architectures, our re-parameterized architecture not only improves the performance of the original network architecture, but also further improves the inference speed of the network. The age function enhances the ability of the algorithm to explore the search space by regularizing the accuracy of the architecture. Experimental data on the benchmark dataset show that our search strategy and the improving reparameterized search space can search for models with better performance.

References

- [1] Redmon J, Divvala S, Girshick R, et al. You only look once: Unified, real-time object detection[C]//Proceedings of the IEEE conference on computer vision and pattern recognition. 2016: 779-788.
- [2] Redmon J, Farhadi A. Yolov3: An incremental improvement[J]. arXiv preprint arXiv:1804.02767, 2018.
- [3] Liu C, Chen L C, Schroff F, et al. Auto-deeplab: Hierarchical neural architecture search for semantic image segmentation[C]//Proceedings of the IEEE/CVF Conference on Computer Vision and Pattern Recognition. 2019: 82-92.
- [4] Fang J, Sun Y, Zhang Q, et al. Fna++: Fast network adaptation via parameter remapping and architecture search[J]. IEEE Transactions on Pattern Analysis and Machine Intelligence, 2020.
- [5] LeCun Y, Bottou L, Bengio Y, et al. Gradient-based learning applied to document recognition[J]. Proceedings of the IEEE, 1998, 86(11): 2278-2324.
- [6] Zhu J Y, Park T, Isola P, et al. Unpaired image-to-image translation using cycle-consistent adversarial networks[C]//Proceedings of the IEEE international conference on computer vision. 2017: 2223-2232.
- [7] Li W, Zhu X, Gong S. Person re-identification by deep joint learning of multi-loss classification[J]. arXiv preprint arXiv:1705.04724, 2017.
- [8] Xiao T, Li S, Wang B, et al. Joint detection and identification feature learning for person search[C]//Proceedings of the IEEE Conference on Computer Vision and Pattern Recognition. 2017: 3415-3424.
- [9] Simonyan K, Zisserman A. Very deep convolutional networks for large-scale image recognition [J]. arXiv preprint arXiv:1409.1556, 2014.
- [10] He K, Zhang X, Ren S, et al. Deep residual learning for image recognition[C]//Proceedings of the IEEE conference on computer vision and pattern recognition. 2016: 770-778.
- [11] Howard A G, Zhu M, Chen B, et al. Mobilenets: Efficient convolutional neural networks for mobile vision applications[J]. arXiv preprint arXiv:1704.04861, 2017.
- [12] Sandler M, Howard A, Zhu M, et al. Mobilenetv2: Inverted residuals and linear bottlenecks[C]//Proceedings of the IEEE conference on computer vision and pattern recognition. 2018: 4510-4520.
- [13] Howard A, Sandler M, Chu G, et al. Searching for mobilenetv3[C]//Proceedings of the IEEE/CVF International Conference on Computer Vision. 2019: 1314-1324.
- [14] Huang G, Liu Z, Van Der Maaten L, et al. Densely connected convolutional networks[C]//Proceedings of the IEEE conference on computer vision and pattern recognition. 2017: 4700-4708.
- [15] Liu H, Simonyan K, Yang Y. Darts: Differentiable architecture search[J]. arXiv preprint arXiv:1806.09055, 2018.
- [16] Hu S, Xie S, Zheng H, et al. Dsnas: Direct neural architecture search without parameter retraining[C]//Proceedings of the IEEE/CVF Conference on Computer Vision and Pattern Recognition. 2020: 12084-12092.
- [17] Cai H, Zhu L, Han S. Proxylessnas: Direct neural architecture search on target task and hardware[J]. arXiv preprint arXiv:1812.00332, 2018.
- [18] Xie S, Zheng H, Liu C, et al. SNAS: stochastic neural architecture search[J]. arXiv preprint arXiv:1812.09926, 2018.
- [19] Lu Z, Whalen I, Boddeti V, et al. Nsga-net: neural architecture search using multi-objective genetic algorithm[C]//Proceedings of the Genetic and Evolutionary Computation Conference. 2019: 419-427.
- [20] Chu X, Zhou T, Zhang B, et al. Fair darts: Eliminating unfair advantages in differentiable architecture search[C]//European conference on computer vision. Springer, Cham, 2020: 465-480.
- [21] Yang Z, Wang Y, Chen X, et al. Cars: Continuous evolution for efficient neural architecture search[C]//Proceedings of the IEEE/CVF Conference on Computer Vision and Pattern Recognition. 2020: 1829-1838.
- [22] Guo Z, Zhang X, Mu H, et al. Single path one-shot neural architecture search with uniform sampling [C]//European Conference on Computer Vision. Springer, Cham, 2020: 544-560.

- [23] Zoph B, Le Q V. Neural architecture search with reinforcement learning[J]. arXiv preprint arXiv:1611.01578, 2016.
- [24] Baker B, Gupta O, Naik N, et al. Designing neural network architectures using reinforcement learning [J]. arXiv preprint arXiv:1611.02167, 2016.
- [25] Pham H, Guan M, Zoph B, et al. Efficient neural architecture search via parameters sharing[C]// International Conference on Machine Learning. PMLR, 2018: 4095-4104.
- [26] Lu Z, Deb K, Goodman E, et al. Nsganetv2: Evolutionary multi-objective surrogate-assisted neural architecture search[C]//European Conference on Computer Vision. Springer, Cham, 2020: 35-51.
- [27] Chen Y, Meng G, Zhang Q, et al. Renas: Reinforced evolutionary neural architecture search [C]//Proceedings of the IEEE/CVF Conference on Computer Vision and Pattern Recognition. 2019: 4787-4796.
- [28] Ding X, Guo Y, Ding G, et al. Acnet: Strengthening the kernel skeletons for powerful cnn via asymmetric convolution blocks[C]//Proceedings of the IEEE/CVF international conference on computer vision. 2019: 1911-1920.
- [29] Ding X, Zhang X, Han J, et al. Diverse Branch Block: Building a Convolution as an Inception-like Unit[C]//Proceedings of the IEEE/CVF Conference on Computer Vision and Pattern Recognition. 2021: 10886-10895.
- [30] Ding X, Zhang X, Ma N, et al. Repvgg: Making vgg-style convnets great again[C]//Proceedings of the IEEE/CVF Conference on Computer Vision and Pattern Recognition. 2021: 13733-13742.
- [31] Zhang M, Yu X, Rong J, et al. RepNAS: Searching for Efficient Re-parameterizing Blocks[J]. arXiv preprint arXiv:2109.03508, 2021.
- [32] Domhan T, Springenberg J T, Hutter F. Speeding up automatic hyperparameter optimization of deep neural networks by extrapolation of learning curves[C]//Twenty-fourth international joint conference on artificial intelligence. 2015.
- [33] Swersky K, Duvenaud D, Snoek J, et al. Raiders of the lost architecture: Kernels for Bayesian optimization in conditional parameter spaces[J]. arXiv preprint arXiv:1409.4011, 2014.
- [34] Lu Z, Deb K, Goodman E, et al. Nsganetv2: Evolutionary multi-objective surrogate-assisted neural architecture search[C]//European Conference on Computer Vision. Springer, Cham, 2020: 35-51.
- [35] Wu B, Dai X, Zhang P, et al. Fbnet: Hardware-aware efficient convnet design via differentiable neural architecture search[C]//Proceedings of the IEEE/CVF Conference on Computer Vision and Pattern Recognition. 2019: 10734-10742.
- [36] Yang Y, You S, Li H, et al. Towards improving the consistency, efficiency, and flexibility of differentiable neural architecture search[C]// Proceedings of the IEEE/CVF Conference on Computer Vision and Pattern Recognition. 2021: 6667-6676.
- [37] Bi K, Xie L, Chen X, et al. Gold-nas: Gradual, one-level, differentiable[J]. arXiv preprint arXiv:2007.03331, 2020.
- [38] Li G, Qian G, Delgadillo I C, et al. Sgas: Sequential greedy architecture search[C]// Proceedings of the IEEE/CVF Conference on Computer Vision and Pattern Recognition. 2020: 1620-1630.
- [39] Yang Y, You S, Li H, et al. Towards improving the consistency, efficiency, and flexibility of differentiable neural architecture search[C]// Proceedings of the IEEE/CVF Conference on Computer Vision and Pattern Recognition. 2021: 6667-6676.
- [40] Real E, Aggarwal A, Huang Y, et al. Regularized evolution for image classifier architecture search [C]//Proceedings of the aaai conference on artificial intelligence. 2019, 33(01): 4780-4789.
- [41] Huang T, You S, Zhang B, et al. DyRep: Bootstrapping Training with Dynamic Re-parameterization[J]. arXiv preprint arXiv:2203.12868, 2022.

Appendix: Model Architecture

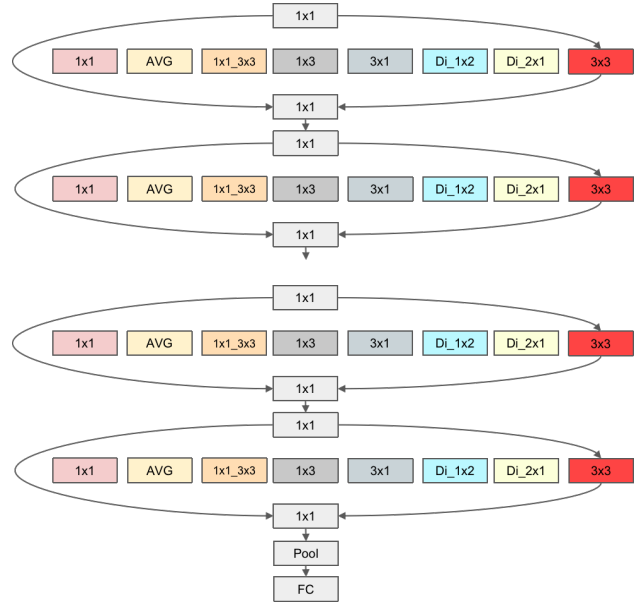
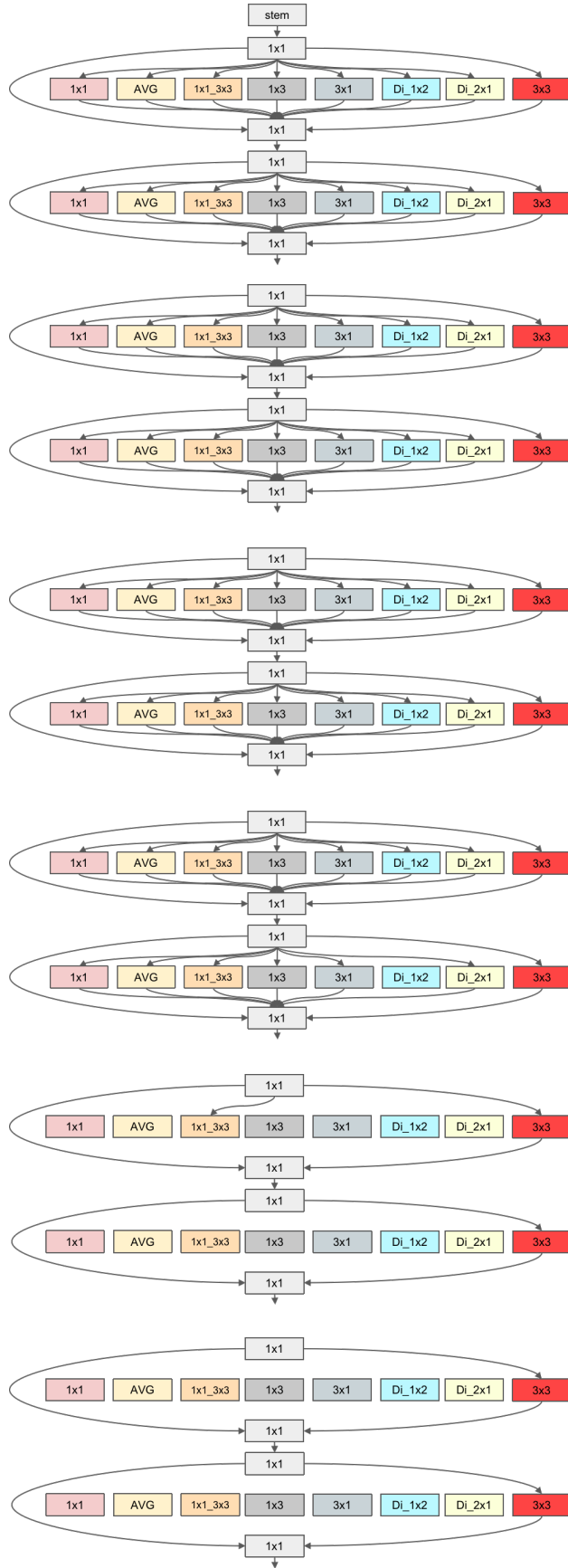


Figure 6. Irep-Resnet50 searched on ImgeNet. The 3×3 convolution operation is a fixed operation and does not participate in the search process of the architecture.